Synthesis and Isolation of Stable Perylenediimide Radical Anion and its Exceptionally Electron-Deficient Precursor

Yogendra Kumar, Sharvan Kumar, Deepak Bansal and Pritam Mukhopadhyay*

School of Physical Science, Jawaharlal Nehru University, New Delhi 110067

Table of Contents

Experimental Details

General: All the chemicals employed in the present work were purchased either from Sigma-Aldrich, Spectrochem India, Loba-Chemie, or Thomas-Baker-India and used as received. PPh_4I was prepared by already reported method.[1] PDI-Br_8 was prepared by our reported method.[2] Thin layer chromatography (TLC) was carried out on aluminum plates coated with silica gel mixed with a fluorescent indicator and was sourced from Merck, Germany. **NMR (^{1}H, ^{13}C)** spectra were recorded on a Bruker 500 MHz spectrometer in CD_3CN and $CDCl_3$ with TMS as a standard. Spin multiplicities are reported as a singlet (s), doublet (d), and triplet (t) with coupling constants (*J*) given in Hz, or multiplet (m). ESI-HRMS spectral data were obtained using a Waters make ESIMS model synaptic G2 high definition mass spectrometry.

Instrumentation and Methods

UV-Vis-NIR and FT-IR Spectroscopy: UV-Vis-NIR spectra were recorded on a JASCO V-670 UV-Vis-NIR Spectrophotometer. All the spectroscopic experiments were carried out in dry UV Grade MeCN, which was sourced from Spectrochem, India. Fourier transform-Infrared spectra in neat were recorded using a Thermo Scientific™ Nicolet™ iS™ 50 FT-IR spectrometer.

Cyclic and Differential Pulse Voltammetry (CV/DPV): CV and DPV studies were carried out using a computer controlled potentiostat (CHI 650C) and a standard three-electrode arrangement that consisted of both platinum working and auxiliary electrodes and saturated calomel (SCE) as a reference electrode. All electrochemical measurements were carried out in Ar-purged DCM with n-Bu_4NPF_6 as the supporting electrolyte. CV measurements were performed with scan rate of 200-300 mV/s. DPV was carried out keeping peak amplitude 50 mV, peak width 0.01 sec, pulse period 0.05 sec and increment E at 20 mV. The working electrode was a platinum gauze working electrode inserted into the quartz cell and the other conditions are the same as those for the cyclic voltammetry. Spectroelectrochemical spectra were recorded on a K-MAC Spectra Academy spectrometer using a thin layer quartz cell (0.5 mm) surmounted with a reference electrode (SCE) and a platinum wire as counter electrode. The working electrode was a platinum gauze working electrode inserted within the quartz cell.

EPR: Electron Spin Resonance (ESR) spectra were recorded using Bruker EMX 1444 EPR spectrometer operating at 9.455 GHz. Diphenylpicrylhydrazyl, DPPH (g = 2.0037), was used for the calibration of ESR spectrometer. The samples were prepared in dry DCM at 5 x 10^{-4} M under inert atmosphere.

Theoretical Calculations: The ground-state geometry optimization was carried out applying the density functional theory (DFT) with the Becke three-parameter[3] hybrid exchange functional in concurrence with the Lee-Yang-Parr gradient-corrected correlation function (B3LYP functional)[4] with the 6-311+G basis set as implemented in Gaussian 09W.[5] All the geometries were optimized without any constrain. To reduce the calculation time axial group (**R′**) of all molecules has been replaced by a methyl group. The electrostatic potentials (ESP) mapped on the electronic density surfaces are based on the DFT calculations and plotted in the Gauss View 5.0 program. To estimate the contributions of the orbitals to the n→π* interaction ($E_{n\rightarrow\pi^*}$) for Br_4CN_4-PDIs, DFT calculations were carried out at the B3LYP/6-311+G level with AIM analysis. The spin density and SOMO were calculated by optimizing the CIF coordinates using DFT CAMB3LYP and LANL2DZ basis sets in gas phase.

X-ray Crystallography: The single crystals of [**1**]$^{\bullet-}$ were grown by slow evaporation of a solution of [**1**]$^{\bullet-}$ in dichloromethane and trifluoro-benzene with a ratio of 2:1 under ambient conditions at ~15 $^{\circ}$C. The crystals were adequately stable under ambient conditions. The reported data sets of all the crystals were collected by mounting the crystal with paratone oil on a loop. X-ray reflections were collected on Bruker D8 Quest diffractometer with CMOS detector using Mo-Kα radiation, generated from the micro-focus sealed tube. Data collection was performed using φ and ω-scans of 0.5° steps at 100 K. Cell determination, data collection, and data reduction were performed with the help of Bruker APEX2 (version: 2.1-b24) software. The structure was solved by intrinsic phasing method (SHELXS-97) and refined by full-matrix least squares refinement method based on F^2, using, SHELXL-2014.[6] The hydrogen atoms were generated with idealized geometries and refined isotropically using a riding model. The crystal structure data are deposited to Cambridge Structural Database with CCDC Number 1883886.

The single crystals of [**2**] were grown by slow evaporation of a solution of [**2**] in MeCN under ambient conditions at RT. The crystals were adequately stable under ambient conditions, losing

the crystalline nature after long exposure to air. The reported data sets of all the crystals were collected by mounting the crystal with paratone oil on a loop. X-ray reflections were collected onBruker D8 Quest diffractometer with CMOS detector using Mo-Kα radiation, generated from the micro-focus sealed tube. Data collection was performed using φ and ω-scans of 0.5° steps at RT. Cell determination, data collection, and data reduction were performed with the help of Bruker APEX2 (version: 2.1-b24) software. The structure was solved by intrinsic phasing method (SHELXS-97) and refined by full-matrix least squares refinement method based on F^2, using, SHELXL-2014. The hydrogen atoms were generated with idealized geometries and refined isotropically using a riding model. The crystal structure data are deposited to Cambridge Structural Database with CCDC Number 1883885.

General Procedure for Synthesis of [1, 2]:

To a 250 mL round-bottom flask 3.139 g (35.2 mmol) of CuCN, 2.0g (1.77 mmol and 1.61 mmol) of respective octa-bromo substituted PDI, and 100 mL of anhydrous dimethylformamide were added. The reaction mixture was stirred under N_2 for 3 h at 80 ˚C. The reaction mixture was cooled to room temperature and poured into 250 mL of distilled water. The precipitate was filtered, washed with water and dissolved in dichloromethane. The solution was dried over $MgSO_4$ and concentrated under reduced pressure. The crude product was purified by column chromatography (silica, chloroform/methanol (90/10) to give an orange-red colour solid of [**1**] or [**2**]. Yield = 0.598 g (37%) for [**1**] and 0.579 g (35%) for [**2**].

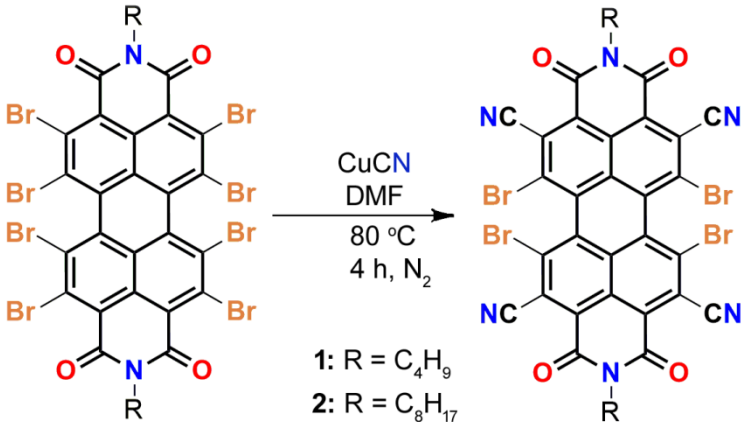

Scheme S1: The synthesis of [**1**] and [**2**].

[**1**]$^{\bullet-}$.PPh_4^+/[**2**]$^{\bullet-}$.PPh_4^+: 300 mg (0.33/0.29 mmol) of the solid product obtained from the 1st step was dissolved in DCM (~50 mL) followed by addition of PPh_4I (~4 eq.) The resulting solution was allowed to stir at room temperature for 30 minutes to afford a green colored solution. Complete electron transfer and formation of radical anion was ensured by UV-Vis-NIR spectroscopy. The reaction mixture was filtered and dried using rotatory evaporator to obtain the green colored radical anion in powder form. Crystallization of the radical anion was done using DCM and 1,2,3 trifluorobenzene in a ratio of (2:1). Yield = 332.0 mg (80%) for [**1**]$^{\bullet-}$.PPh_4^+ and 310.0 mg (78%) for [**2**]$^{\bullet-}$.PPh_4^+: [All the operations were performed under ambient conditions].

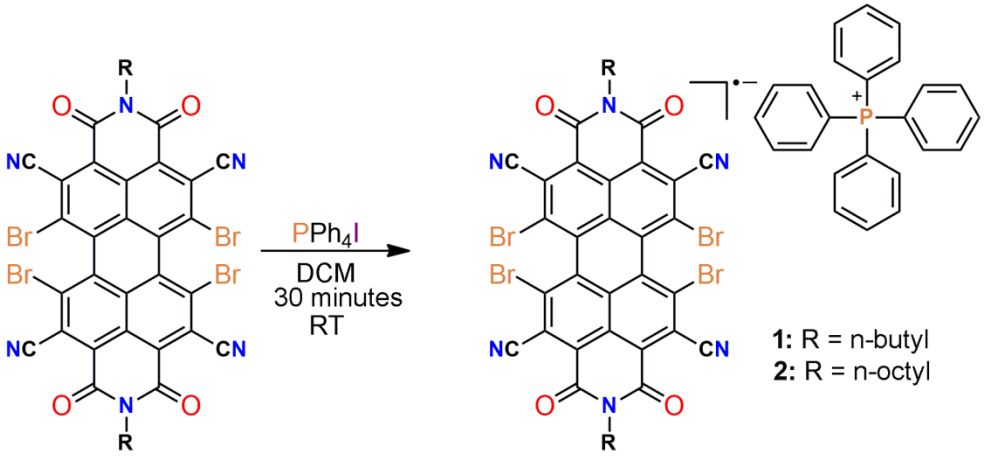

Scheme S2: Synthesis of PDI-radical anions.

[**1**]$^{2-}$/[**2**]$^{2-}$: 200 mg (0.22/0.19 mmol) of the solid product obtained from the 1st step was dissolved in CH_3CN (~50 mL) followed by addition MeOH solution of Na_2S (~2 eq.) The resulting solution was allowed to stir at room temperature for 5 minutes to afford a blue colored solution. Complete electron transfer and formation of dianion was ensured by UV-Vis-NIR spectroscopy. The reaction mixture was filtered and dried using rotatory evaporator to obtain the blue colored dianion in powder form. Yield = 191.0 mg (90%) for [**1**]$^{2-}$ and 180.0 mg (88%) for [**2**]$^{2-}$. [All the operations were performed under ambient conditions].

Synthesis of [1]: N,N-dibutyl-1,6,7,12-tetrabromo-2,4,8,11-tetracyano-perylene-3,4,9,10-tetracarboxylic acid bisimide. Yield = 0.598 g (37%). Melting point > 300 $^{\circ}$C. Solubility: soluble in CH_2Cl_2 and MeCN. ^{1}H NMR (500 MHz, $CDCl_3$, TMS, 298 K): δ (ppm) = 4.32 (t, 4H, J = 7.5 Hz), 1.29-1.27 (m, 8H, J = 7.5 Hz), 1.03 (t, 6H, J = 7.5 Hz). ^{13}C NMR (125 MHz, $CDCl_3$, TMS):

δ (ppm) = 139.29, 131.89, 130.31, 114.45, 114.07, 42.23, 31.93, 29.51, 25.62, 22.70, 20.33, 14.12. MS (ESI-HRMS): Calculated for $C_{36}H_{18}N_6O_4$ 918.18, found 918.18. FT-IR (neat): $\bar{\nu}$ (cm^{-1}) = 2957, 2928, 2867, 2228, 1710, 1668, 1566, 1354, 1207 cm^{-1}. Anal. Calcd. for $C_{40}H_{18}N_{10}O_4$: C 47.09, H 1.98, N 9.15; Found: C 46.97, H 1.95, N 9.21.

[1$^{\bullet-}$].PPh$_4^+$: Yield = 332.0 mg (80%). MS (ESI-HRMS): Calculated for $C_{36}H_{18}N_6O_4$ 918.1819, found 918.8109. FT-IR (neat): $\bar{\nu}$ (cm^{-1}) = 2951, 2924, 2862, 2221, 1668, 1640 1545, 1475, 1306, 1102 cm^{-1}.

[1]$^{2-}$: Yield = 191.0 mg (90%). ^{1}H NMR (500 MHz, CD_3CN, TMS, 298 K): δ (ppm) = 4.23 (t, 4H, *J* = 7.5 Hz), 1.73-1.67 (m, 4H, *J* = 7.5 Hz), 1.48-1.44 (m, 4H, *J* = 7.5 Hz), 1.03 (t, 6H, *J* = 7.5 Hz). ^{13}C NMR (125 MHz, $CDCl_3$, TMS): δ (ppm) = 39.95, 20.28, 13.35. MS (ESI-HRMS): Calculated for $C_{36}H_{18}N_6O_4$ 918.18, found 918.18. FT-IR (neat): $\bar{\nu}$ (cm^{-1}) = 2954, 2924, 2864, 2216, 1616, 1550, 1302 cm^{-1}.

Synthesis of [2]: N,N-octyl-1,6,7,12-tetrabromo-2,4,8,11-tetracyano-perylene-3,4,9,10-tetracarboxylic acid bisimide. Yield = 0.579 g (35%). Melting point > 300 $^\circ$C. Solubility: soluble in $CHCl_3$ and MeCN. ^{1}H NMR (500 MHz, $CDCl_3$, TMS, 298 K): δ (ppm) = 4.30- 4.26 (t, 4H, *J* = 7.5 Hz), 1.79 (4H, *J* = 7.5 Hz), 1.60 (4H, *J* = 7.5 Hz), 1.43-1.39 (16H, *J* = 7.5 Hz), 0.91 (t, 6H, *J* = 7.5 Hz). ^{13}C NMR (125 MHz, $CDCl_3$, TMS): δ (ppm) = 160.49, 159.14, 137.75, 132.60, 131.62, 129.66, 128.41, 126.42, 123.49, 118.59, 114.94, 42.36, 31.79, 29.39, 28.00, 27.48, 22.71, 22.65, 15.75. MS (ESI-HRMS): Calculated for $C_{44}H_{34}Br_4N_6O_4$ 1030.39, found 1029.83. FT-IR (neat): $\bar{\nu}$ (cm^{-1}) = 2954, 2923, 2854, 2223, 1710, 1668, 1560, 1345, 1191 cm^{-1}. Anal. Calcd. for $C_{44}H_{34}Br_4N_6O_4$: C 51.29, H 3.33, N 8.16; Found: C 51.45, H 3.45, N 8.24.

[2$^{\bullet-}$].PPh$_4^+$: Yield = 310.0 mg (78%). Calculated for $C_{36}H_{18}N_6O_4$ 1030.3945, found 1030.2233. FT-IR (neat): $\bar{\nu}$ (cm^{-1}) = 2950, 2920, 2850, 2219, 1670, 1637 1545, 1480, 1436, 1306, 1107 cm^{-1}.

[2]$^{2-}$: Yield = 180.0 mg (88%).$^{-1}$H NMR (500 MHz, CD_3CN, TMS, 298 K): δ (ppm) = 4.25-4.13 (t, 4H, *J* = 7.5 Hz), 1.83-1.82 (m, 4H, *J* = 7.5 Hz), 1.73-1.61 (m, 20H, *J* = 7.5 Hz), 1.03 (t, 6H, *J* = 7.5 Hz). ^{13}C NMR (125 MHz, CD_3CN, TMS): spectrum could not be recorded due to the poor solubility. MS (ESI-HRMS): Calculated for $C_{36}H_{18}N_6O_4$ 1030.3945, found 1030.2233. FT-IR (neat): $\bar{\nu}$ (cm^{-1}) = 2953, 2918, 2851, 2216, 2063, 1617, 1558, 1424, 1310, 1127 cm^{-1}.

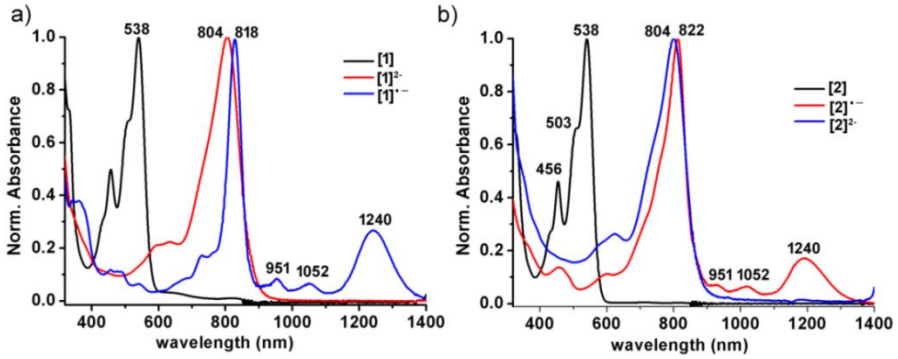

Figure S1: Normalized UV-Vis-NIR absorption spectra of a) [**1**], [**1**]$^{\bullet-}$ and [**1**]$^{2-}$ and b) [**2**], [**2**]$^{\bullet-}$ [**2**]$^{2-}$ in DCM.

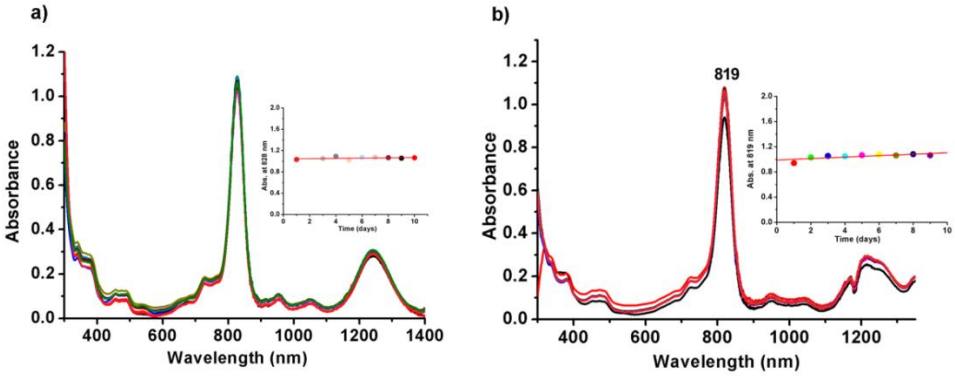

Figure S2: Time-dependent UV-vis-NIR spectra of [**1**$^{\bullet-}$]**.PPh$_4^+$** at 5 × 10^{-5} M under ambient conditions in a) DCM and b) THF:H_2O (90:10); and inset figure shows the stability of [**1**$^{\bullet-}$]**.PPh$_4^+$**.

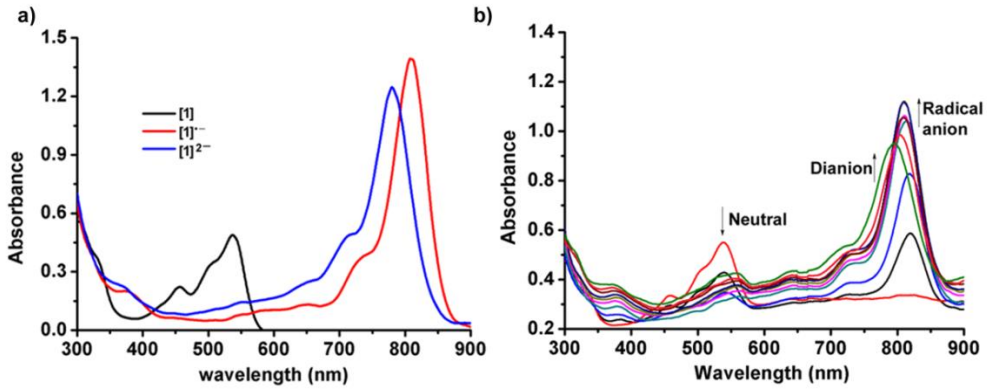

Figure S3: (a) UV-vis-NIR absorption changes upon electrochemical reduction spectra of **1** to [**1**$^{\bullet-}$] at -0.16V potential and [**1**$^{\bullet-}$] to [**1**]$^{2-}$ at - 1V potential. (b) UV-vis-NIR absorption changes upon electrochemical reduction spectra of **2** to [**2**$^{\bullet-}$] at -0.16V potential for 10 minutes and [**2**$^{\bullet-}$] to [**2**]$^{2-}$ at -1V potential for 5 minutes.

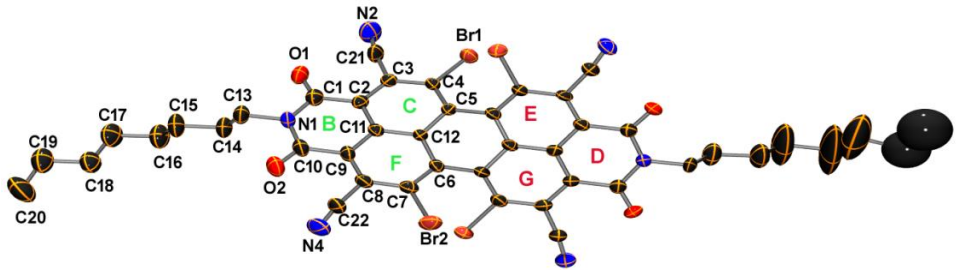

Figure S4: ORTEP representation of crystal [**2**] (ellipsoids are drawn at 50% probability). The H atoms and solvent molecules have been removed for clarity.

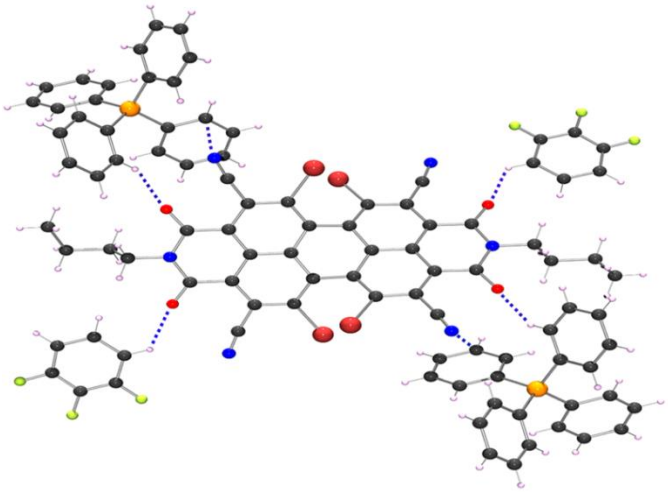

Figure S5: Showing the hydrogen bonding interactions of **[1]** $^{\bullet-}$ with **PPh**$_4^+$ and solvent molecules.

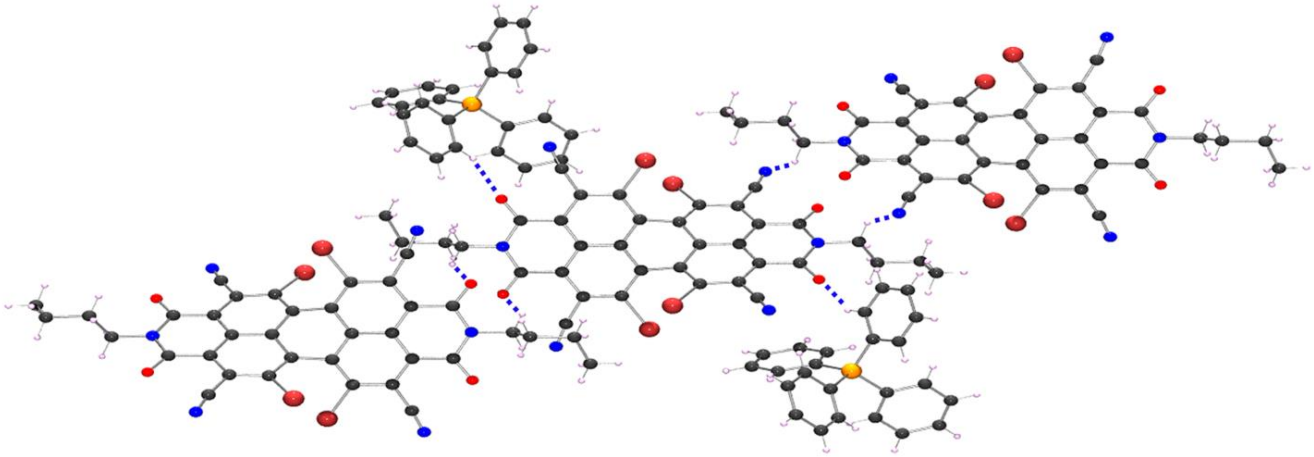

Figure S6: Showing intermolecular C≡N---H and C=O---H hydrogen bonding interactions.

Table S1: Comparison of the selected bond lengths and angles of the crystal structure and geometry optimized structures of [(**1**$^{\bullet-}$)·PPh_4^+] and [**2**].

Entry	Selected Bond length [Å] Crystal Data			Selected Bond length [Å] B3LYP 6-311 +G	
	Atoms	[**1**$^{\bullet-}$]	[**2**]	[**1**]	[**1**$^{\bullet-}$]
1	C1─O1	1.222	1.191	1.242	1.253
2	C10─O2	1.220	1.215	1.243	1.253
3	C1─N1	1.136	1.379	1.400	1.405
4	C10─N1	1.401	1.405	1.397	1.401
5	C1─C2	1.465	1.493	1.482	1.463
6	C2─C3	1.407	1.370	1.397	1.417
7	C3─C4	1.391	1.416	1.423	1.402
8	C4─C5	1.398	1.382	1.401	1.419
9	C5─C12	1.412	1.425	1.435	1.432
10	C12─C6	1.411	1.430	1.435	1.432
11	C6─C7	1.412	1.386	1.401	1.419
12	C7─C8	1.394	1.414	1.423	1.402
13	C8─C9	1.397	1.349	1.397	1.416
14	C9─C10	1.464	1.488	1.480	1.462
15	C2─C11	1.403	1.410	1.418	1.418
16	C9─C11	1.417	1.409	1.418	1.418
17	C11─C12	1.422	1.411	1.422	1.432

18	C17≡N2	1.156	1.139	1.165	1.166
19	C18≡N3	1.145	1.132	1.165	1.166
20	C4—Br1	1.902	1.872	1.936	1.949
21	C7—Br2	1.896	1.882	1.936	1.949
	Selected bond angles (°)				
22	C3—C17≡N2	172.87°	172.46	175.49	175.44
23	C8—C18≡N3	172.94°	173.45	175.61	175.55
	Selected torsions bond angle(°)				
24	C(4) -C(5) -C(6')-C(7')	-	41.84	34.33	29.19
25	C(4')-C(5')-C(6)-C(7)	-	39.29	- 34.32	-29.19

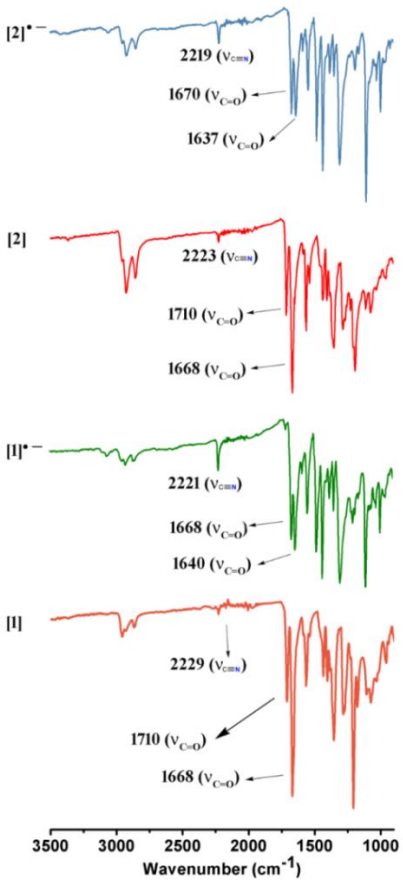

Figure S7: FT-IR spectrum of compound [**1**], [**1**$^{\bullet-}$]**.PPh**$_4^+$, [**2**] and [**2**$^{\bullet-}$]**.PPh**$_4^+$**.**

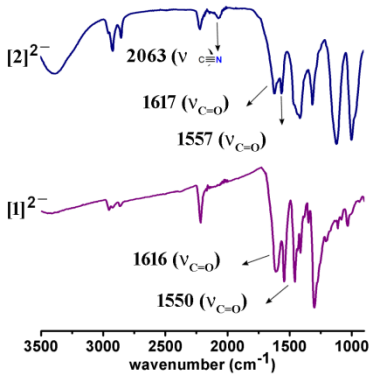

Figure S8: FT-IR spectrum of $[\mathbf{1}]^{2-}$ and $[\mathbf{2}]^{2-}$.

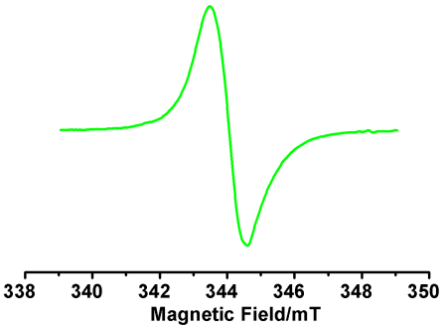

Figure S9: Solid state EPR spectrum of $[\mathbf{1}^{\bullet-}]\mathbf{.PPh_4}^{+}$ at 295 K.: Microwave frequency 9.663 GHz; microwave power 0.805 mW; receiver gain 2 x 10^2; modulation frequency 100 kHz; modulation amplitude 1.00 G. g value = 2.0072.

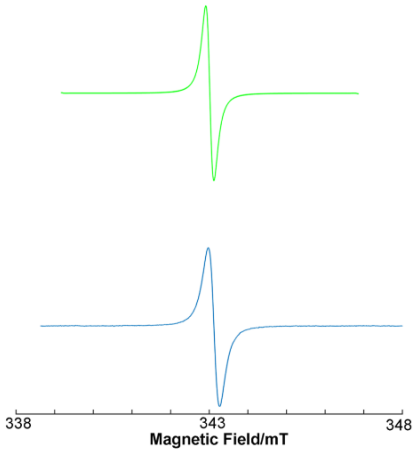

Figure S10: EPR (bottom) and simulated (top) spectra for $[\mathbf{2}^{\bullet-}]$ in DCM at 295 K.: Microwave frequency 9.634 GHz; microwave power 6.471 mW; receiver gain 1.59 x 10^2; modulation frequency 100 kHz; modulation amplitude 0.30 G.

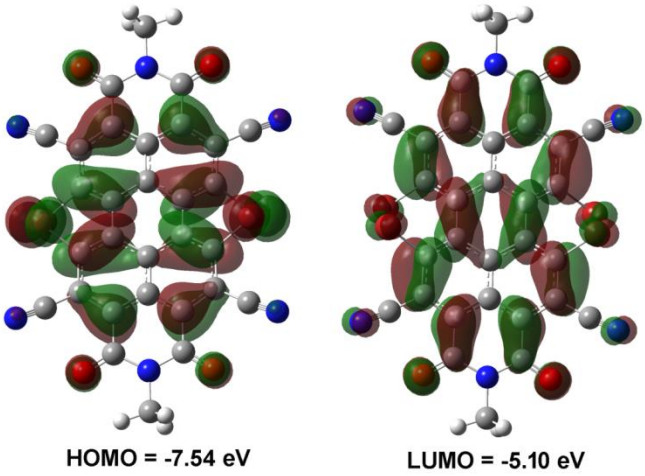

Figure S11: Frontier molecular orbital diagram of [PDI-Br_4CN_4]. For finding the HOMO-LUMO surface contours, structures were optimized by DFT calculation at B3LYP/6-311+G basis set.

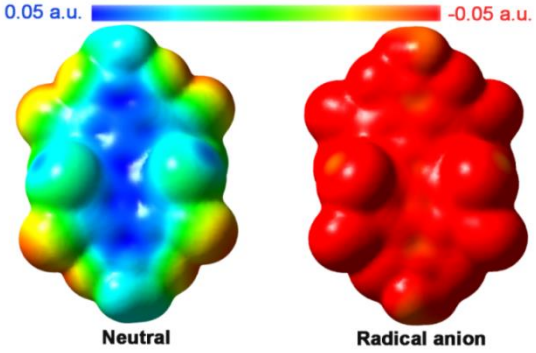

Figure S12: ESP maps of the neutral and radical anion of PDI-Br_4CN_4**.** The contours are color-coded from red (electron rich) to blue (electron deficient).

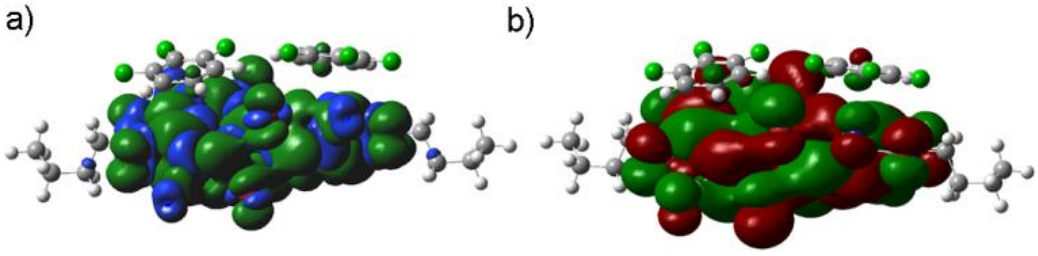

Figure S13: a) Spin density (isovalue = 0.0001 e–/au^3) and b) SOMO (isovalue = 0.005 e–/au^3) of the geometry optimized [(**1**$^{\bullet-}$) 1,2,3-triflourobenzene] in the gas phase using DFT CAMB3LYP and LANL2DZ.

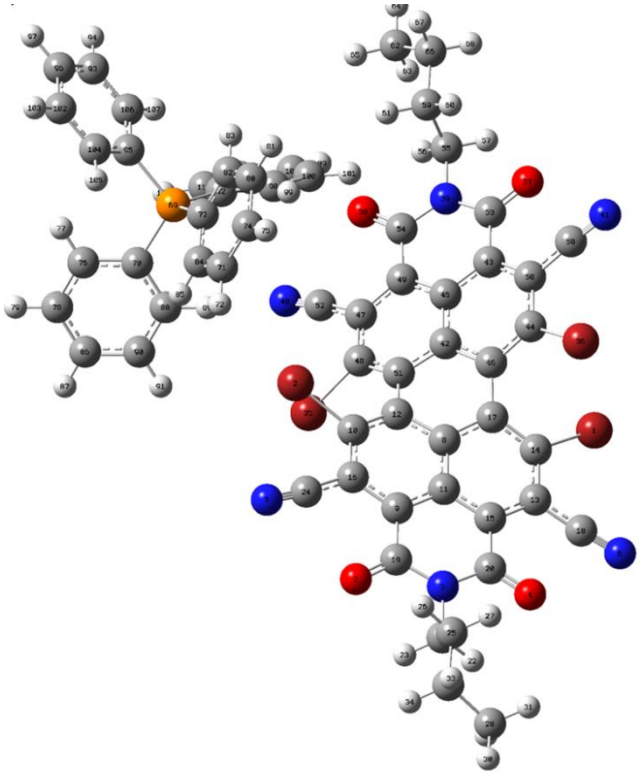

Table S2: Calculated Mulliken charges and Spin density distributions of the [(**1**•−).PPh_4^+] at 6311+G basis set (selected atoms) [Atom numbering is provided with the structure, page S13]:

	[(**1**•−).PPh_4^+]	
Atoms	Mulliken charges	Spin densities
Br1	-0.06003	0.010288
Br2	-0.21527	0.009915
O3	-0.19124	0.048070
O4	-0.16677	0.047216
N5	0.225335	-0.006293
N6	-0.13877	-0.000359
N7	-0.17608	-0.002411
C8	-0.01172	0.012708
C9	0.327207	0.128782
C10	-0.37836	0.092106
C11	0.008607	-0.037072
C12	0.402923	-0.012268
C13	1.068553	-0.015294
C14	-0.54594	0.075769
C15	0.416592	0.113236
C16	1.098393	-0.028116
C17	0.38081	-0.015277
C18	-1.18969	0.000463
C19	-0.36267	-0.008727
C20	-0.40511	-0.008907
C24	-0.91249	0.003558
C42	0.024787	-0.019252
C43	0.415665	0.102529
C44	-0.3467	0.051201
C45	0.009887	-0.026425
C46	0.334272	0.058436
C47	0.620268	0.030055
C48	-0.79762	0.024228
C49	0.184273	0.123457
C50	1.056783	0.027146
C51	0.385619	0.079246
C52	-0.27101	-0.006494
C53	-0.5115	-0.001027
C54	-0.44333	0.005539
C58	-1.0729	-0.012143
Br35	-0.00128	0.008131
Br36	-0.08023	0.009813
O37	-0.16735	0.059298
O38	-0.19131	0.057486
N39	0.301571	-0.011664
N40	-0.03055	0.018245
N41	-0.15244	0.017036
C74	-0.17499	-0.003258

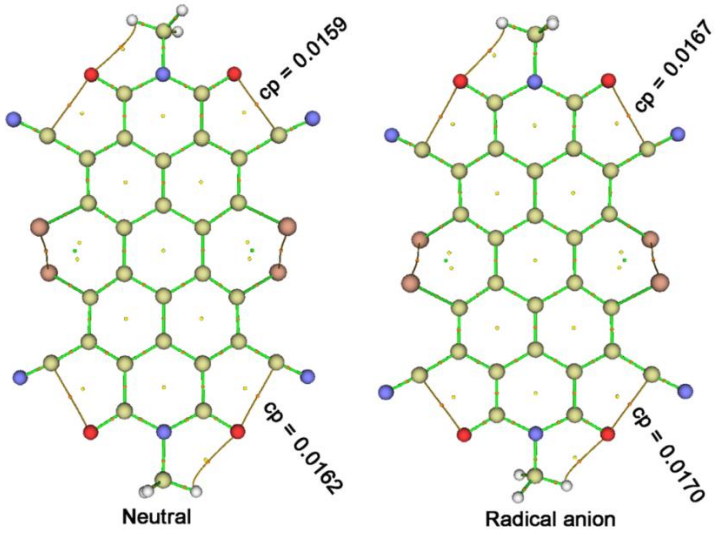

Figure S14: 3D molecular diagram representing C---O interaction in neutral PDI-Br_4CN_4 (left) and PDI-Br_4CN_4 radical anion (right).

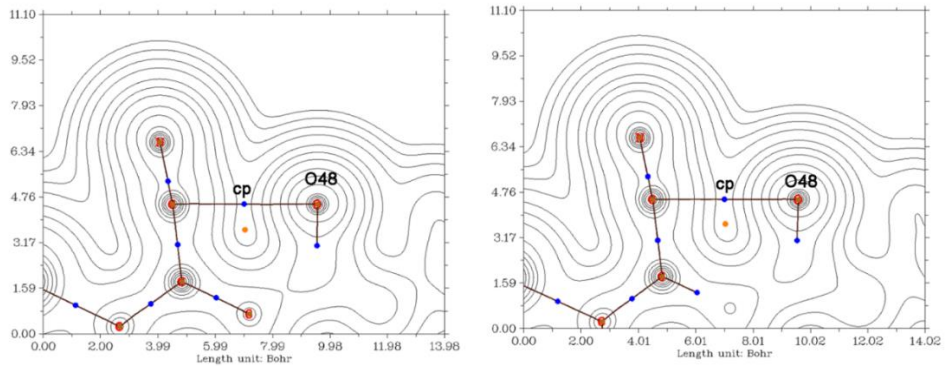

Figure S15: 2D contour plot showing the bond path between C and O atom in neutral PDI-Br_4CN_4 (left) and PDI-Br_4CN_4 radical anion (right).

Table S3: AIM parameters for neutral PDI-Br_4CN_4 and radical anion of PDI-Br_4CN_4 molecules.

Entry	Bond	$\rho(\mathbf{r}_b)^b$	$\nabla^2\rho(\mathbf{r}_b)^c$	$E(\mathbf{r}_b)^d$	$G(\mathbf{r}_b)^e$	$V(\mathbf{r}_b)^f$
1	C1---O1	0.0170	0.0609	0.0013	0.0132	-0.0124
1$^{\bullet-}$	C1---O1	0.0162	0.0577	0.0013	0.0131	-0.0117

[a]Theoretical topological properties at the BCPs; values from a 6-311+G basis set. [b]The electron density at BCP. [c]Laplacian of electron density. [d]The electron energy density. [e]Kinetic energy electron density. [f]Potential energy electron density. All are in a.u.

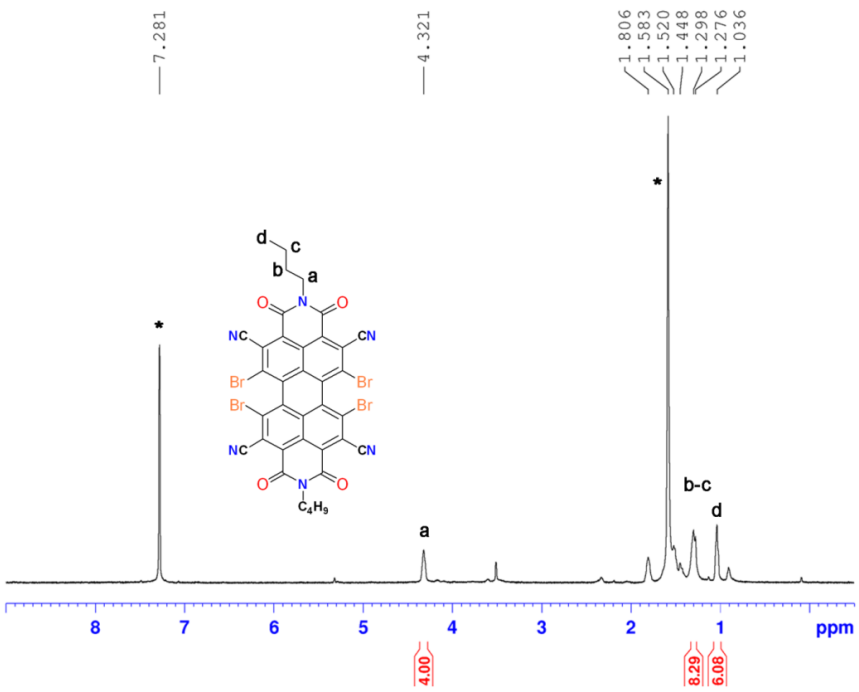

Figure S16: 500 MHz ^{1}H NMR spectrum of **[1]** in $CDCl_3$ at room temperature. Number of scans (NS = 64). *residual solvent peak.

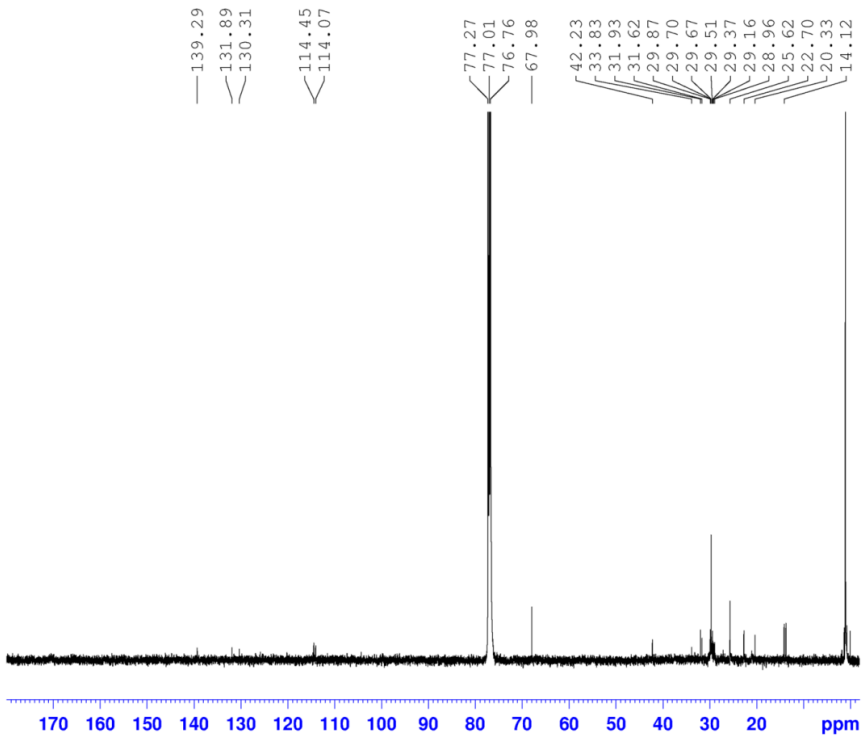

Figure S17: 125 MHz ^{13}C spectrum of **[1]** in $CDCl_3$ at room temperature.

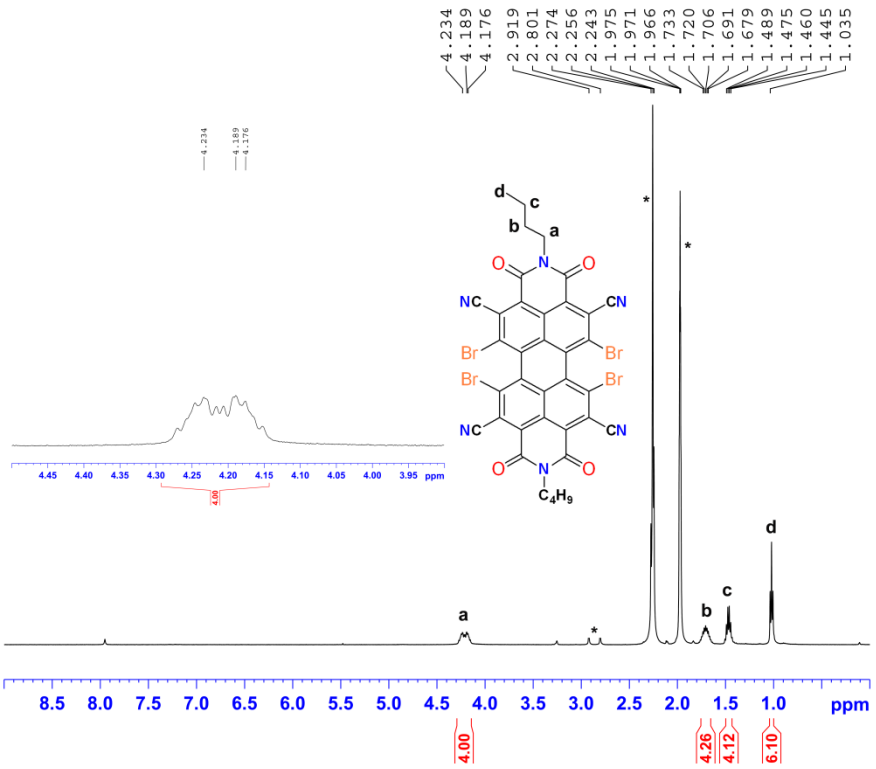

Figure S18: 500 MHz ^{1}H NMR spectrum of [**1**]$^{2-}$ in CD_3CN at room temperature. Number of scans (NS = 32). *residual solvent peak.

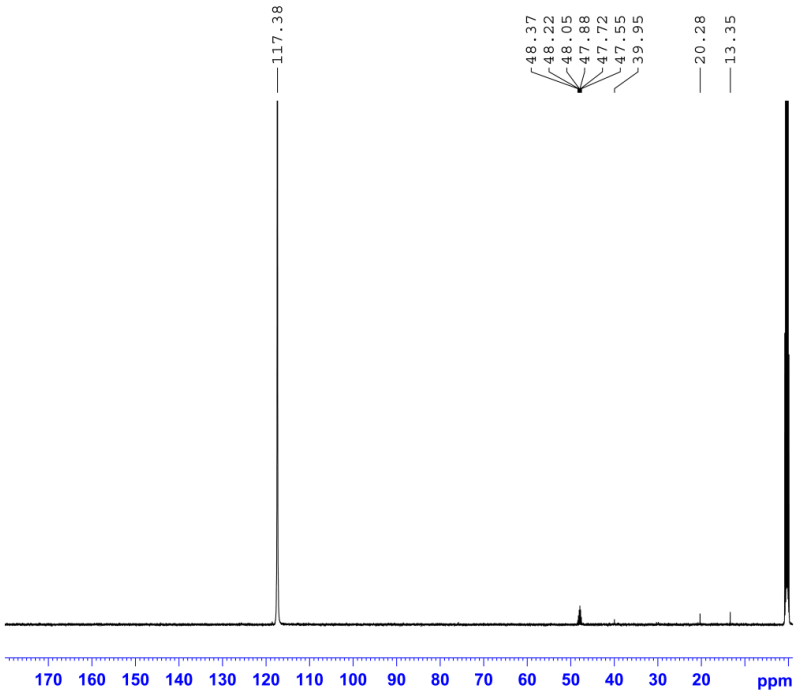

Figure S19: 125 MHz ^{13}C spectrum of [**1**]$^{2-}$ in CD_3CN at room temperature.

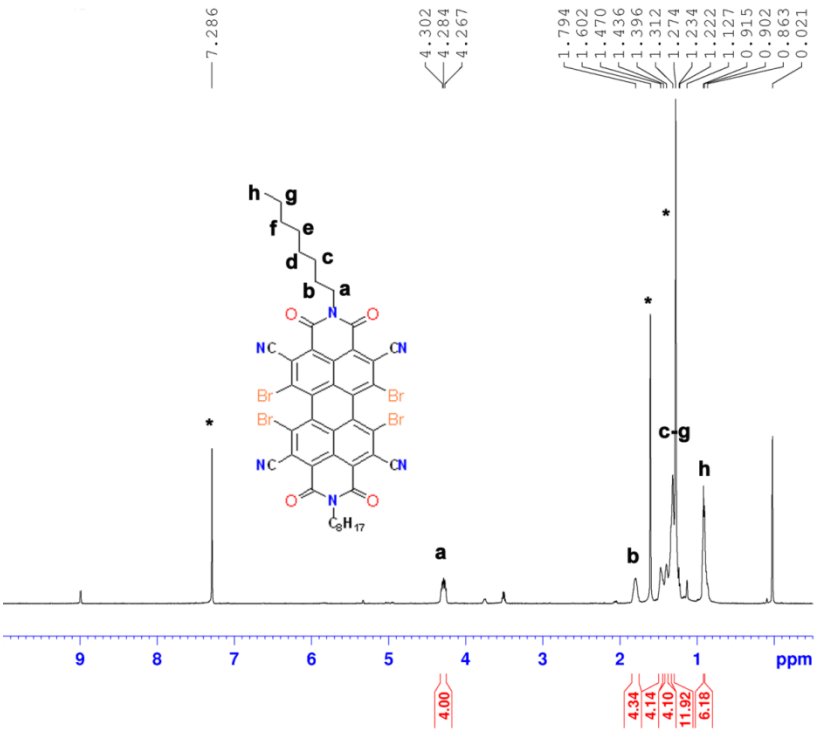

Figure S20: 500 MHz ^{1}H NMR spectrum of **[2]** in $CDCl_3$ at room temperature. Number of scans (NS = 160). * residual solvent peak.

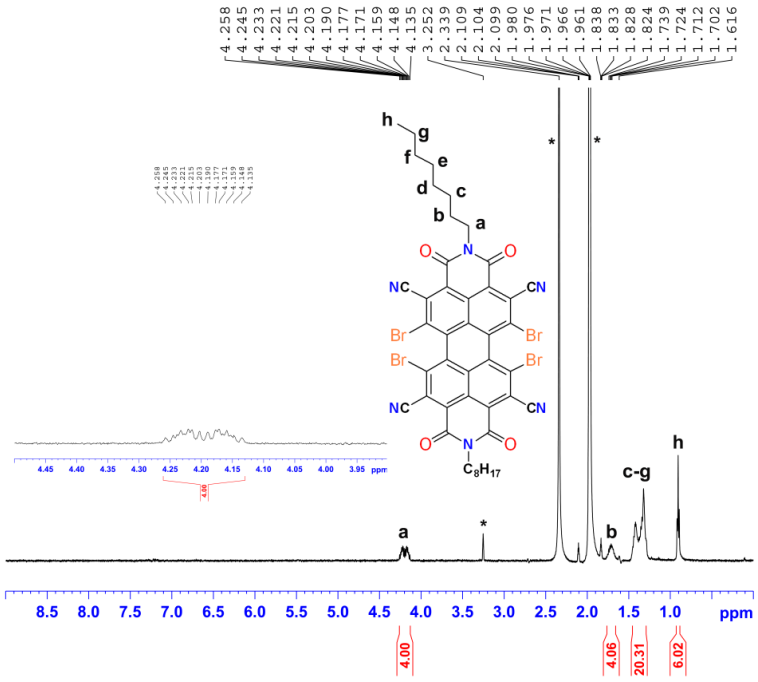

Figure S21: 500 MHz ^{1}H NMR spectrum of $[\mathbf{2}]^{2-}$ in CD_3CN at room temperature. Number of scans (NS = 64). *residual solvent peak.

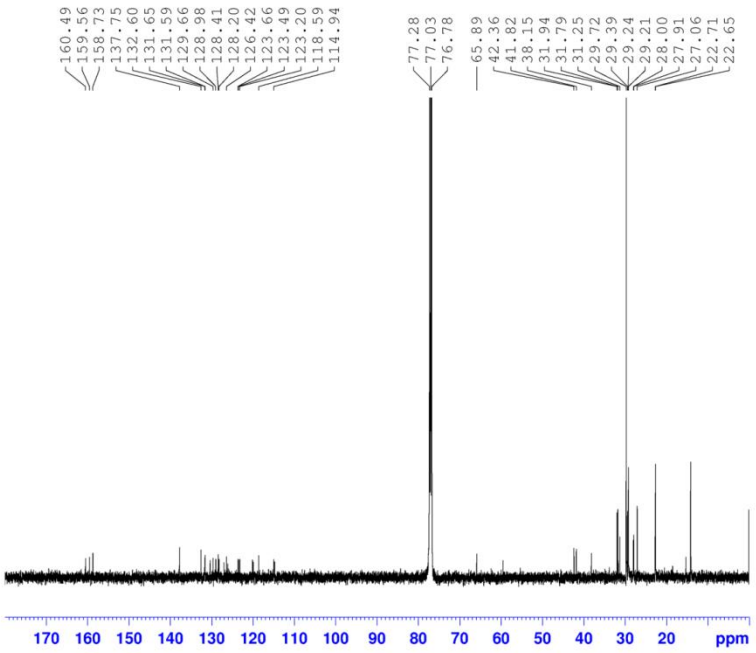

Figure S22: 125 MHz ^{13}C spectrum of [**2**] in $CDCl_3$ at room temperature.

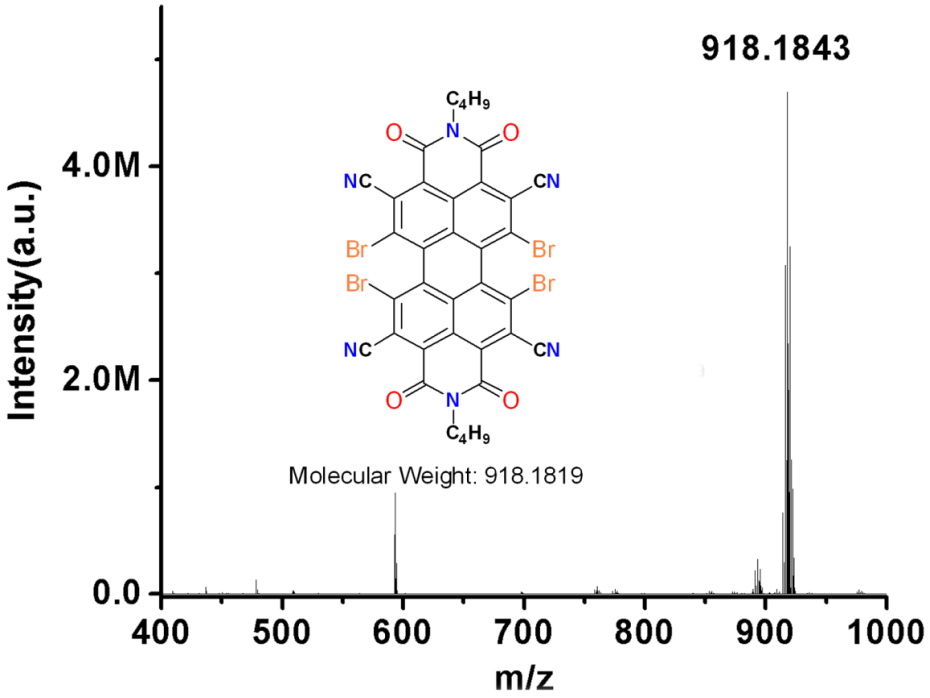

Figure S23: HRMS-ESI mass spectrometry of [**1**].

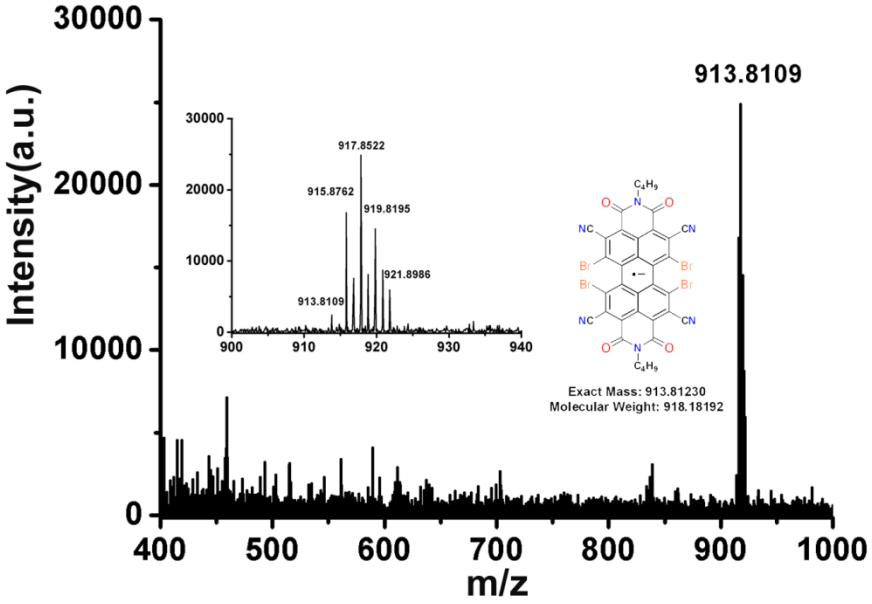

Figure S24: HRMS-ESI mass spectrometry of [(**1**•−).PPh_4^+].

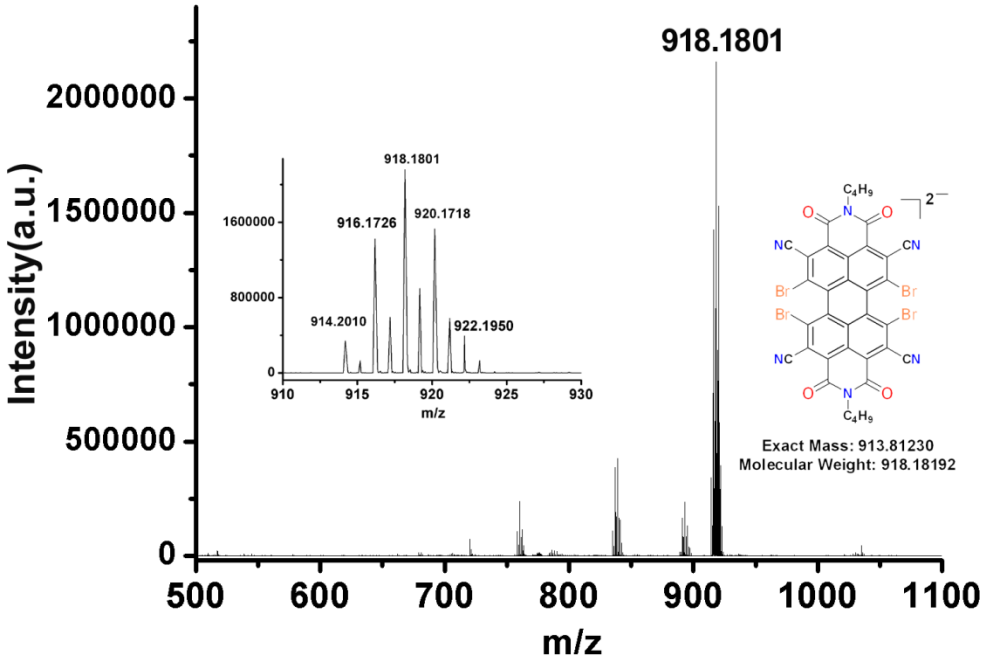

Figure S25: HRMS-ESI mass spectrometry of $[\mathbf{1}]^{2-}$.

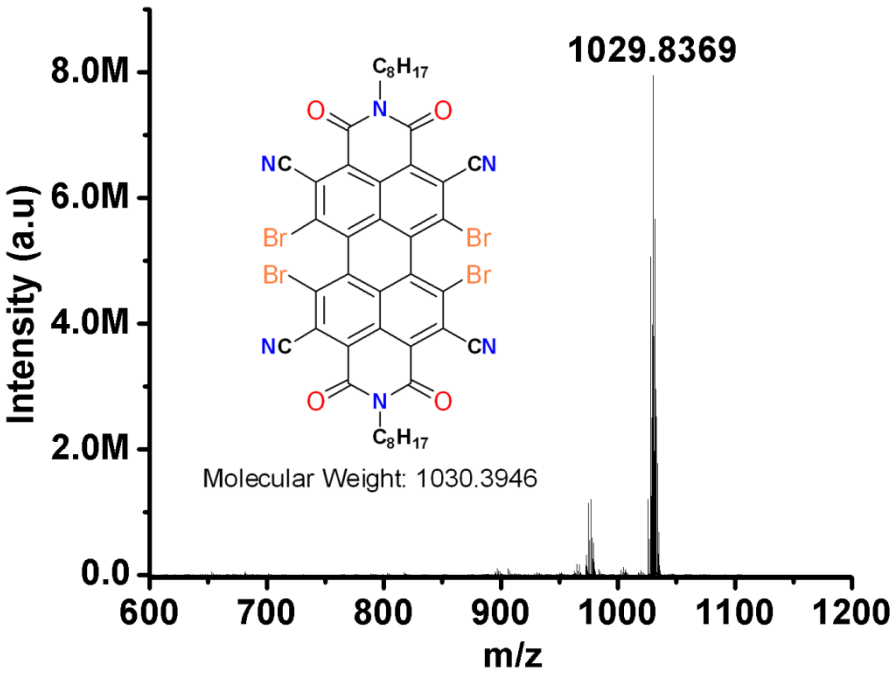

Figure S26: HRMS-ESI mass spectrometry of [**2**].

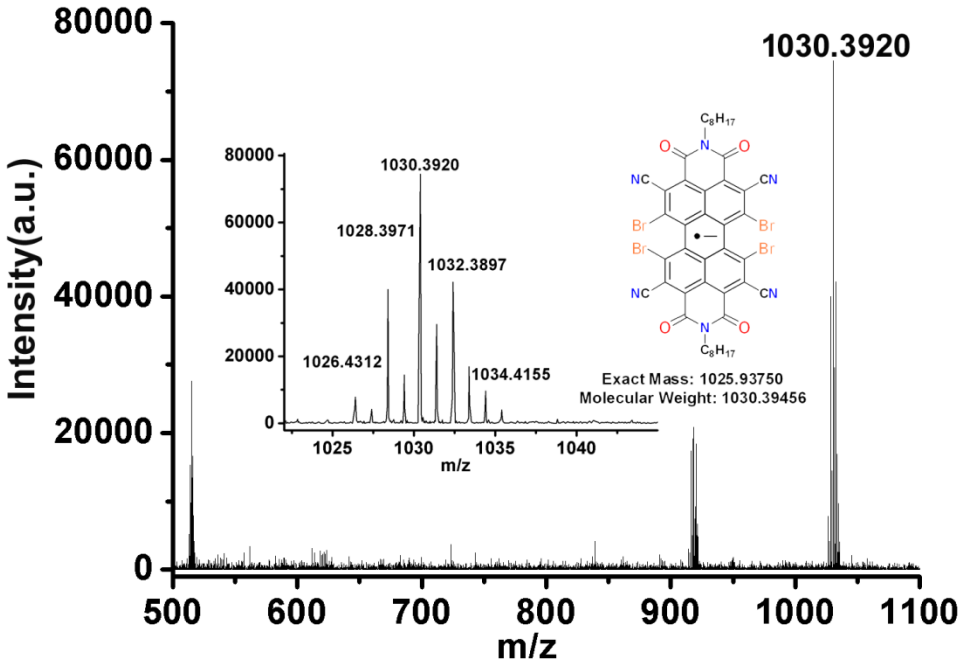

Figure S27: HRMS-ESI mass spectrometry of [(**2**•−).PPh_4^+].

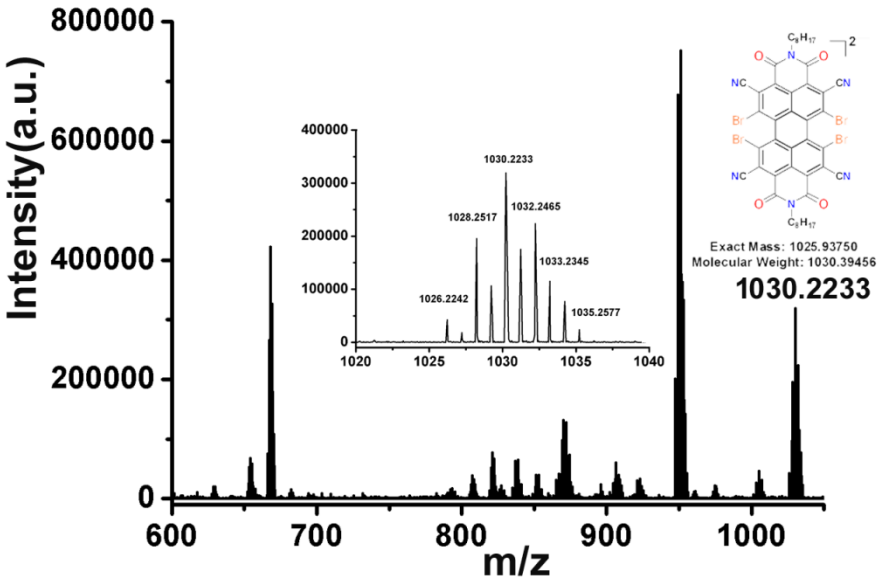

Figure S28: HRMS-ESI mass spectrometry of $[\mathbf{2}]^{2-}$.

References:

1. T. Migita, T. Nagai, K. Kiuchi and M. Kosugi, *Bull. Chem. Soc. Jpn.* **1983**, *56*, 2869.
2. Y. Kumar, S. Kumar, S. K. Keshri, J. Shukla, S. S. Singh, T. S. Thakur, M. Denti, A. Facchetti and P. Mukhopadhyay, *Org. Lett.* **2016**, *18*, 472.
3. A. D. Becke, *J. Chem. Phys.* **1993**, *98*, 5648.
4. C. Lee, W. Yang and R. G. Parr, *Phys. Rev. B* **1988**, *37*, 785.
5. Gaussian 09, Revision D.01, M. J. Frisch, G. W. Trucks, H. B. Schlegel, G. E. Scuseria, M. A. Rob, J. R. Cheeseman, G. Scalmani, V. Barone, B. Mennucci, G. A. Petersson, H. Nakatsuji, M.; Li, X. Caricato, H. P. Hratchian, A. F. Izmaylov, J. Bloino, G. Zheng, J. L. Sonnenberg, M. Hada, M. Ehara, K. Toyota, R. Fukuda, J. Hasegawa, M. Ishida, T. Nakajima, Y. Honda, O. Kitao, H. Nakai, T. Vreven, Jr. J. A. Montgomery, J. E. Peralta, F. Ogliaro, M. Bearpark, J. J. Heyd, E. Brothers, K. N. Kudin, V. N. Staroverov, R. Kobayashi, J. Normand, K. Raghavachari, A. Rendell, J. C. Burant, S. S. Iyengar, J. Tomasi, M. Cossi, N. Rega, J. M. Millam, M. klene, J. E. Knox, J. B. Cross, V. Bakken, C. Adamo, J. Jaramillo, R. Gomperts, R. E. Startmann, O. Yazyev, A. J. Austin, R. Cammi, C. Pomelli, J. W. Ochterski, R. L. Martin, K. Morokuma, V. G. Zakrzewski, G. A. Voth, P. Salvador, J. J. Dannenberg, S. Dapprich, A. D. Daniels, Ö. Farkas, J. B.

Foresman, J. V. Ortiz, J. Cioslowski and D. J. Fox, *Gaussian, Inc.*, Wallingford CT, **2009**.

6. G. M. Sheldrick, *Acta Crystallogr. Sect. A* **2008**, 64, 112.